Fabrication of an aluminum–carbon nanotube metal matrix composite by accumulative roll-bonding

S. Salimi · H. Izadi · A. P. Gerlich

Abstract Accumulative roll-bonding was adapted to fabricate a carbon nanotube (CNT)-reinforced aluminum matrix composite. Its microstructure was investigated by transmission electron microscopy, and it was confirmed that the nanotubes were embedded into the metal matrix while maintaining their multiwalled structure. Measurements revealed that the as-received CNTs had a bimodal diameter size distribution, while only nanotubes with diameters >30 nm and >30 walls were retained during four consecutive rolling operations at 50% reduction.

Introduction

Accumulative roll-bonding was developed by Saito et al. [1] as a severe plastic deformation technique for refining the grain size of an alloy. In this process multiple layers of metals or alloys are stacked together and then rolled until a sufficient degree of deformation is achieved and a solid-state bond between the original individual metal pieces is formed. To form the bond, sufficient pressure on the metal strips should be applied and a threshold strain value should be achieved [2].

This deformation facilitates grain refinement to the nanocrystalline range, and therefore a high degree of strengthening can be achieved using ARB in various kinds of steels and aluminum alloys [3–5]. Laminated composites of alternating metal layers may be fabricated by the ARB process, and this has been demonstrated with foils of Ni and Zr [6], Al and Ni [7], as well as Ni, Ti, and Zr [8].

In some cases it was possible to produce a laminated sheet with nanocrystalline or even amorphous microstructure [6, 8]. The total reduction applied on the material may be limited due to embrittlement with increasing work hardening; however, ductile materials can be roll bonded to exceptionally high total strains [3].

A variation of the roll-bonding process has been developed in which a nanoscale powder reinforcing material is dispersed between the sheets prior to rolling, with the aim of producing a layer of metal matrix composite material at the interface. The process is similar to sheath-rolling which has been discussed elsewhere [9]; however, it does not require reheating or vacuum encapsulation of the sheets. Fabrication of composites by roll-bonding has been demonstrated using Al sheets and SiO_2 particles [10], Cu foils and single-walled carbon nanotubes (CNTs) [11], and Al foils with multiwalled CNTs [12]. In all cases the layered composites exhibited both increased strength and stiffness due to the exceptional properties of the CNTs [13–15]. These structural enhancements may be realized in a metal matrix composite and potentially also offer improved electrical and thermal properties [16–18], since multiwalled CNTs may also exhibit superconducting properties [19].

The fabrication steps involved are summarized in Fig. 1. This process has the advantage of increasing the strength of the matrix material via grain refinement, and has the potential to achieve high concentrations of CNT material in the composite since the process has the potential to be repeated for several passes by changing the parameters of the process. It should also been noted that it has been proposed that reinforcing fibers are dispersed and preferentially aligned in the rolling direction during roll-bonding of CNT metal matrix composites [11, 12]. Also the rate of entanglement in the CNT base material may be reduced

S. Salimi · H. Izadi · A. P. Gerlich (✉)
Department of Chemical and Materials Engineering,
University of Alberta, Edmonton, AB T6G 2V4, Canada
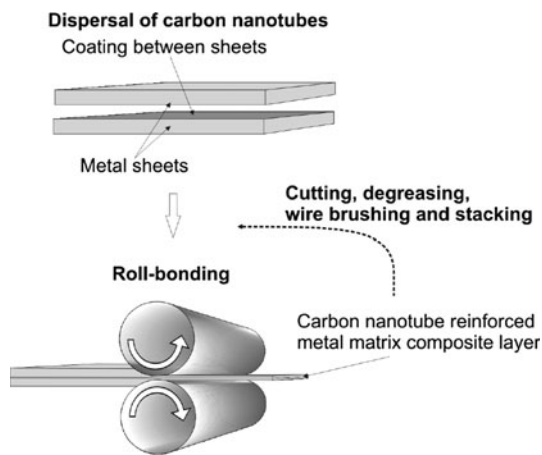e-mail: gerlich@ualberta.ca

Fig. 1 Schematic illustration of the composite fabrication process via accumulative roll-bonding

during fabrication using this process, particularly with increased strains during repeated rolling operations.

Although a great deal of success has been achieved in synthesizing polymer–CNT composites, producing metal matrix CNT composites is rather challenging. However, some techniques have included hot extrusion, equal channel angular pressing, shockwave consolidation, and mechanical alloying [20–22]. The use of CNTs as a reinforcement has been shown to provide improved properties in various metal matrix composites [23–25]; however, a number of challenges need to be considered during synthesis. For example, the processing route may result in damage of the nanotube structure, poor interfacial bonding between CNTs and metal matrix, or agglomeration of the CNTs [26]. Sintering of metal powders with CNTs at high temperature may promote chemical reaction of nanotubes with the surrounding matrix, although this may be detrimental to the properties of the CNT [27]. Although possible damage to the CNTs has been suggested during roll bonding of Al–CNT composite [12], the factors controlling the CNT stability during the process have never been examined. This is a particular concern since potential to distribute the CNTs more uniformly by repeated ARB cycles depends on their stability or resistance to rupture with subsequent passes, and this issue is addressed in this study.

Experimental

The sheet material used during roll-bonding was a commercial pure aluminum alloy (AA1100) with a composition of Al–0.51Fe–0.13Cu–0.08Si–0.03Mn. The as-received aluminum consisted of a fully annealed microstructure with an equiaxed average grain size of 52 μm, and was cut into $150 \times 25 \times 1.4$ mm³ strips. Multiwalled CNTs were

ultrasonically agitated in 2-propanol, and then heated in order to evaporate the alcohol and obtain a highly concentrated suspension of CNTs. After degreasing the aluminum and wire brushing the surfaces, the sheets were coated once with the concentrated CNT suspension and allowed to dry. The sheets were then stacked together making a 2.8-mm-thick sandwich that was accumulatively roll-bonded four times at room temperature with intermediate degreasing and wire brushing as indicated in Fig. 1. The diameter of the rollers was 100 mm, the rolling speed was 75 rpm, and the thickness reduction was 50% during each pass. It should be noted that the aluminum sheets were only coated with CNT material once in order to determine the influence of mechanical loading on nanotubes all exposed to the same number of rolling cycles.

TEM was used to study the microstructure of the metal matrix composite. The TEM samples were prepared from 3-mm disks which were punched out from the plan view of the sheet and mechanically thinned. These were then electropolished using a solution of 25 vol.% of HNO_3 and 75 vol.% of methanol at a temperature of -35 °C and voltage of 12 V, and examined using a JEOL 2010 microscope operating at 200 kV. Samples which were observed along the transverse plane of the sheet were sectioned using electrical discharge machining before electropolishing.

Results and discussion

Aluminum matrix and CNT microstructures

Figure 2 shows the morphology of the as-received CNTs, which ranged in diameter from 10 to 70 nm, and a nominal axial length of 10–20 μm. Due to their length and morphology, the as-received CNT material was highly entangled.

The microstructure of the CNTs and matrix grains in the composite material following four rolling passes are shown in Figs. 3 and 4. The repeated rolling cycles produced an ultra fine-grained matrix consisting of high-angle boundaries with grain sizes ranging from 100 to 500 nm in the rolling direction. However, in the normal direction (ND) of the sheet, the grains with thicknesses of <100 nm could readily be observed, with an average grain thickness after four cycles of 109 nm (see Fig. 4b). This is finer than the equilibrium thickness of 0.4 μm previously reported for Al 3003 [28]; however, this may be expected since this study utilizes a higher strain rate during roll-bonding. The grains were not completely equiaxed and exhibited some elongation in the rolling direction.

Continuous rings are present in the diffraction pattern of Fig. 3a, corresponding with the CNT base material.
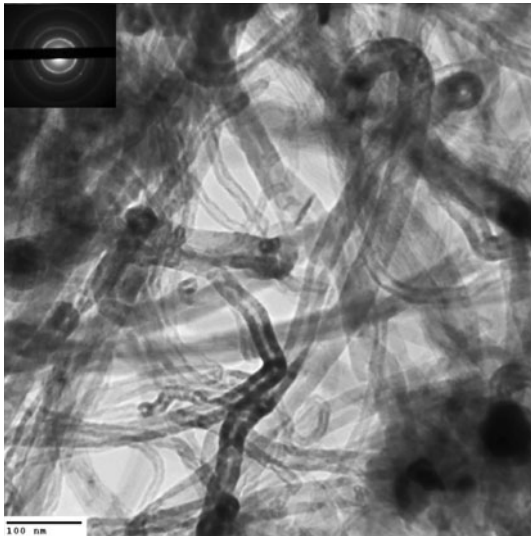
Fig. 2 TEM micrograph of the as-received multiwalled CNT material

In addition, the spot patterns observed in the selected area diffraction pattern correspond with two grains in Fig. 3a with orientations of {200} and {222}, indicating a high angle grain boundary misorientation exists between them. It has already been shown that during roll bonding of aluminum, the deformation imposed during one rolling pass with a 50% reduction is only sufficient to produce a subgrain structure, where low-angle boundaries (with misorientations <15°) dominate between grains [4]. The subgrain structure remains after two cycles, but the dislocation density increases. Following three roll-bonding cycles the dislocation density is dramatically reduced and grains show broad contours within them that suggest high internal stress [29]. At this stage subgrains are still dominant; however, some of their boundaries are well developed and have large misorientations. An ultra fine-grained structure with primarily high-angle grain boundaries becomes dominant after four cycles of roll-bonding. This ultra fine-grained microstructure is indicated by the dense and nearly continuous distribution of spots in the diffraction patterns [4], which is consistent with the selected diffraction pattern shown in Fig. 3a. The combination of accumulative roll-bonding differs from previous studies of roll-bonding alloy sheets with CNT powders, since the final structure was not repeatedly rolled a minimum of four passes each at 50% reduction, otherwise the final matrix structure will consist primarily of subgrains [11, 12].

Due to non-uniform strain distributions which may occur during rolling [30], the distribution of high-angle grain boundaries and grain thickness may vary depending on the thickness location [31–33]. Typically, larger shear strains are produced in the near surface region, and this effect is particularly enhanced when no lubrication is used during rolling [34]. As a result, the grain size is typically finer near the surface due to a higher amount of shear strain, resulting in a larger amount of accumulated dislocations and grain subdivision [33]. Clearly, the strain gradient and strain path during deformation play an important role in the formation of geometrically necessary dislocations and ultra fine grain sizes [35–37].

In the case of ARB, the shear strain localized at the surface of any individual pass is distributed during subsequent stacking or folding operations, hence the distribution of deformation eventually becomes uniform with increasing number of cycles. However, the grain size is also influenced by recrystallization and growth resulting due to an adiabatic temperature rise during rolling [33].
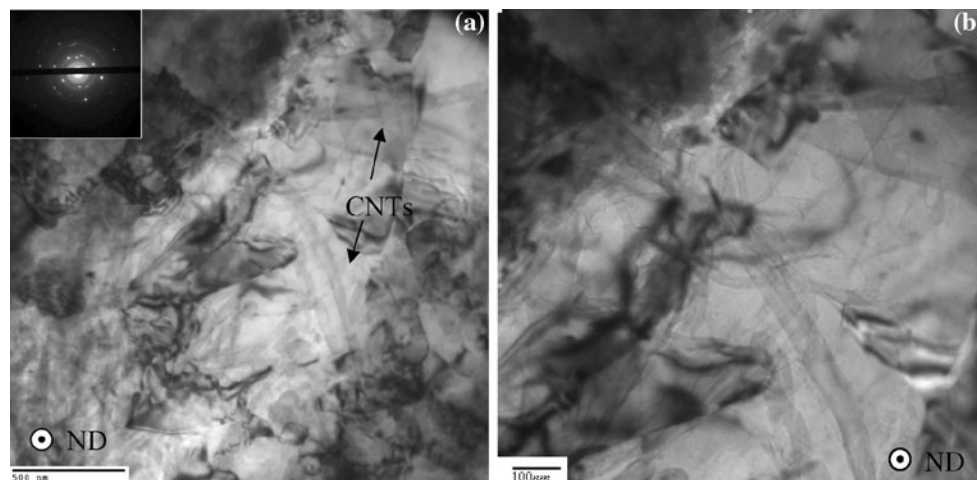

Fig. 3 TEM micrograph of **a** the roll-bonded CNT-reinforced aluminum composite layer with selected area diffraction pattern when viewed along the ND of the sheet, and **b** the individual CNTs in the matrix
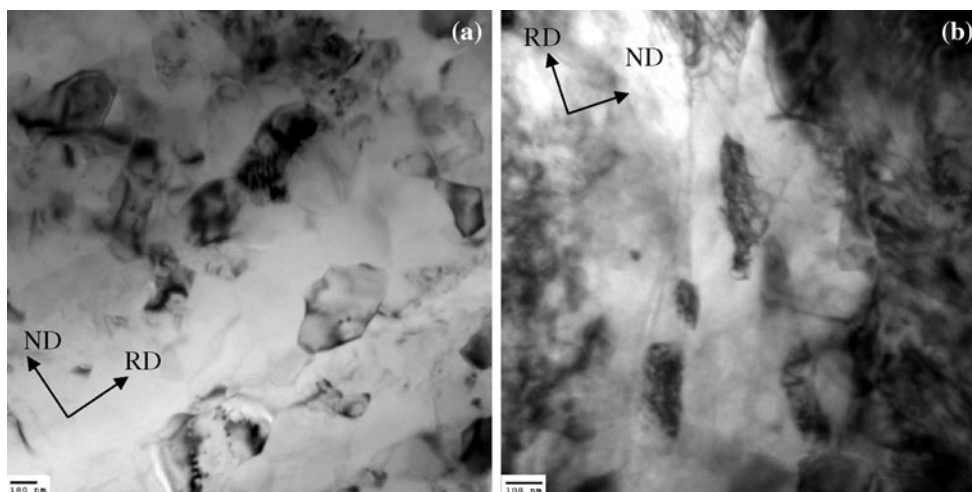
Fig. 4 TEM micrograph of the cross section of the roll-bonded CNT-reinforced aluminum composite material after four passes
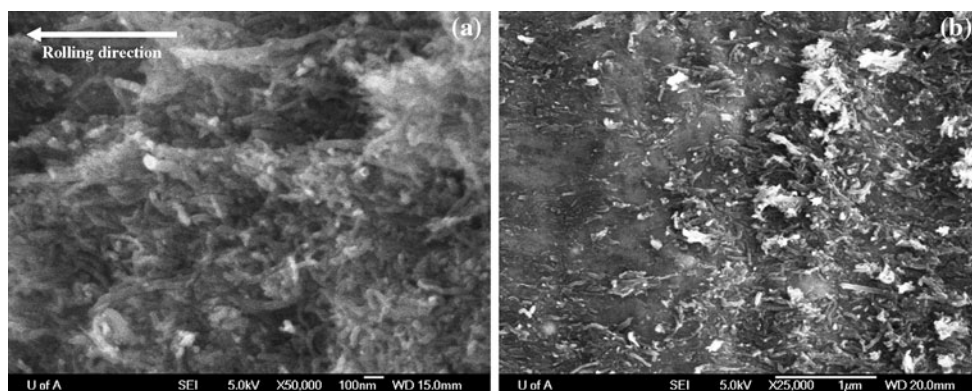

Fig. 5 SEM image of the interface of the roll-bonded composite sheets after they were mechanically delaminated

Consequently, although ARB is useful in achieving a more uniform structure through the thickness of the sheet, there may ultimately be a limiting grain size for a given material regardless of how many passes are imposed.

The average measured *d*-spacing values for the three continuous diffraction rings observed in Fig. 3a were 3.50, 2.11, and 1.22 Å, which are within 1% of the spacing values observed for the (002), (004), and (110) Miller indices of the hexagonal unit cell suggested by Keller et al. [38] for CNTs. The first and most intense ring corresponds well with the reflections observed for the graphene spacing found in multiwalled CNTs [38], confirming that these are present in the composite. EDX analysis was conducted on Fig. 3b revealed strong Al and C peaks for the composite material.

CNT orientation and adhesion at the interface

The properties of CNTs are dependant on their orientation, and so this was investigated by mechanically delaminating

the sheets following roll-bonding, and observing the CNTs dispersed between the sheets. This was done by mechanically delaminating and peeling apart the sheets following three cycles of roll-bonding operation using a sharp blade to open the strongly bonded interface and examining the surface using SEM, as shown in Fig. 5. The surface revealed a non-uniform distribution of CNTs which were mostly aligned flat to the surface of the sheet. Although the CNTs were more dispersed than in the as-received material, some entangled bundles of CNTs could also be observed (see Fig. 5b). There was also evidence of aluminum fracture surfaces created by the delamination, since metallic bonding between the aluminum sheets is promoted during roll-bonding.

Since the delamination process may disrupt the CNTs from their original orientation, a cross section was also heavily etched with HF to expose the CNTs. The sheet interfaces are revealed due to preferential etching, allowing removal of the aluminum material from the sheet interfaces and avoiding mechanical disruption their arrangement.
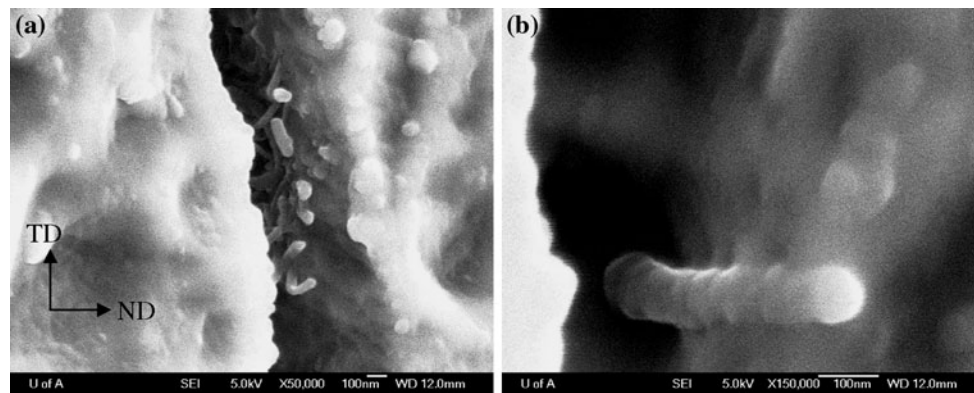
Fig. 6 SEM image of **a** the cross section of the reinforced layer in the roll-bonded CNT-reinforced aluminum composite material following etching with HF, and **b** a single CNT embedded in the aluminum

Figure 6a shows the CNTs at the interface, with the majority of CNTs axially aligned in the RD or TD directions. Some of the CNTs were observed to emerge from the aluminum matrix, indicating that there was intimate contact promoted between the CNTs and the aluminum (see Fig. 6b). This suggests that adhesion has been promoted in-between the surrounding matrix.

Rupture of CNTs during rolling

By optimizing the distribution of CNTs and uniformity of the matrix microstructures demands repetitive rolling of the sheets. A highly uniform distribution of nanotubes in the through-thickness direction provided that CNTs are only introduced once before the initial rolling cycle, and several cycles are applied. For example, since the number of reinforced layers increases exponentially during repeated processing, the number of CNT-reinforced layers is equal to $(2^n - 1)$, where n is the number of roll-bonding cycles. Hence, the resistance of the CNTs to rupture is a key feature to achieving a uniform distribution of reinforcement in the final composite.

Alternatively, another key feature of the ARB fabrication process is that it may permit the concentration of CNTs to be increased by repeatedly producing an additional reinforced layer between the stacked sheets prior to each rolling cycle. A prerequisite for the fabrication process is for the majority of nanotubes to remain intact during repeated rolling in order to achieve a satisfactory yield in the final bulk composite. To assess the integrity of the CNTs during rolling, the diameters were measured for 110 nanotubes in the as-received material, as well as for 117 nanotubes subjected to 4 rolling cycles, using the TEM micrographs.

The as-received CNTs clearly exhibit a bimodal size distribution in terms of their diameters (see Fig. 7). This may occur depending on the synthesis route taken to
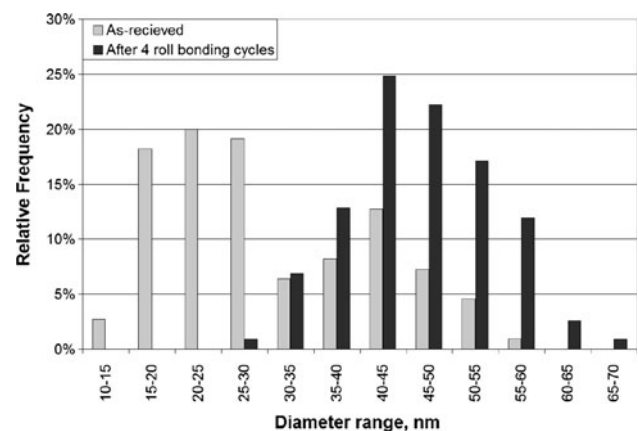

Fig. 7 Distribution of CNT diameters in the as-received material and roll-bonded aluminum metal matrix composite. The number of samples measured was 110 and 117 for the as-received and roll-bonded CNT populations, respectively

fabricate the multiwalled CNTs [39]. Although no CNTs with diameter range of 60–70 were observed in the as-received CNTs, this does not mean that they were not present. The sample size of 100 may not be sufficient to capture the population with these diameters (which therefore likely comprised less than 1% of the CNTs in the as-received material). Following four roll-bonding cycles, the CNTs with diameters approximately >30 nm appear to have been retained in the composite. Multiwalled CNTs with larger diameters may sustain larger strains when subjected to radial compression [17, 40]. In addition, the larger CNTs in the base material also tended to have a higher apparent wall thickness (see Fig. 8a), which indicates that these consisted of a greater number of walls. It has been shown using continuum mechanics that the critical buckling stress during radial loading of a multiwalled CNT will increase with the number of walls since the pressure is more evenly distributed over a greater number of walls [41]. As show in Fig. 6, one can assume that the

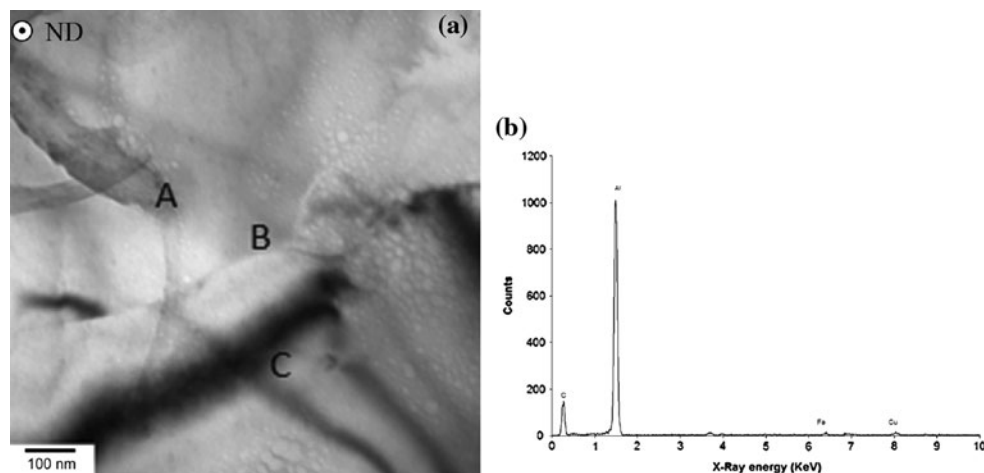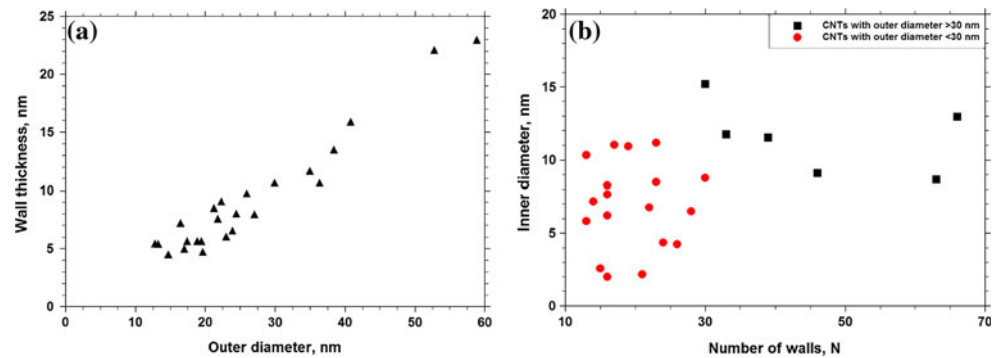**Fig. 8** Diameter and wall thickness measurements for the CNT base material

Fig. 9 a TEM micrograph of the roll-bonded composite with the end of a broken CNT at A, and **b** EDX spectrum of the sample at point A

primary loading condition during rolling is compressive loading along the radial direction of the CNTs. Consequently, it is not surprising that the population of CNTs which survived most readily is those which have greater wall numbers, corresponding with those that also had outer diameters >30 nm (see Fig. 8b).

However, one other property of multiwalled CNTs is that the radial buckling stress of the CNTs should increase as the inner diameter decreases [41]. In contrast the CNTs which had a smaller inner radius did not survive the loading cycles during rolling in this study. It is possible that this may be accounted for by the biaxial loading conditions imposed during rolling. Due to the mismatch in the yield strength and stiffness of CNTs versus aluminum, CNTs are exposed to high axial tensile stresses during the rolling process. Shen and Zhang [42] have shown that under combined axial and radial loading multiwalled CNTs will buckle sooner than when only radial force is applied. Therefore, the axial tensile stress which contributes to buckling is lower in CNTs with a larger diameter since these have a higher number of walls and there is a greater effective cross-sectional area. Under the same loading conditions during rolling, there will be more pressure on

Table 1 EDX quantification (in at.%) measured at points A–C of Fig. 9

Point	Al	C	Si	Fe	Cu	Ca
A	68.0	30.8	0	0.4	0.8	0
B	76.6	18.1	0	0.1	0.8	4.4
C	94.3	2.2	0.1	0.6	0.9	1.9

CNTs having smaller diameter. The buckling process is a precursor to rupture of the CNTs since the formation of kinks and defects occurs during buckling [43], ultimately leading to failure. Hence, the CNTs which have prematurely buckled are not likely to survive the rolling process.

Evidence of ruptured CNTs could be found by using TEM and EDX analysis. The chemical composition was measured at the three points showing in Fig. 9 and the results are given in Table 1. A progressively decreasing fraction of carbon could be detected at points further from the end of the broken CNT. The carbon content at point C could correspond to carbon in solution locations of the aluminum matrix devoid of CNTs, though it should also be noted that the distance between points A and C is on the

order of the interaction volume, and the carbon quantification is on the limit detection by EDX. However, in previous studies it has been shown that the results of these ruptures would be formation of highly defected carbon structures such as graphite layers [44], these may dissociate into the aluminum matrix and form a solid solution with carbon contents similar to that observed in point C in Fig. 9. It is suggested that this carbon was contributed primarily by the CNTs with diameters <30 nm that ruptured during rolling.

Conclusion

It has been shown that a modification of the accumulative roll-bonding may be used to disperse CNTs into an aluminum alloy. The process was effective in producing a composite microstructure with multiwalled CNTs embedded in an ultra fine-grained aluminum matrix. The CNTs with diameters >30 nm and more than 30 walls readily endured four consecutive roll-bonding operations, and their multiwalled structure was preserved in the final composite.

References

1. Saito Y, Utsunomiya H, Tsuji N, Sakai T (1999) Acta Mater 47:579
2. Vaidyanath LR, Nicholas MG, Milner DR (1959) Br Weld J 6:13
3. Tsuji N, Saito Y, Lee SH, Minamino Y (2003) Adv Eng Mater 5:338
4. Saito Y, Tsuji N, Utsunomiya H, Sakai T, Hong RG (1998) Scripta Mater 39:1221
5. Tsuji N, Saito Y, Utsunomiya H, Tanigawa S (1999) Scripta Mater 40:795
6. Hsieh PJ, Lo YC, Huang JC, Ju SP (2006) Intermetallics 14:924
7. Min GH, Lee JM, Kang SB, Kim HW (2006) Mater Lett 60:3255
8. Dinda GP, Rosner H, Wilde G (2005) Scripta Mater 52:577
9. Mizuuchi K, Inoue K, Yamauchi K, Enami K, Itami M, Okanda Y (2001) Mater Sci Eng A Struct 316:93
10. Lu C, Tieu K, Wexler D (2009) J Mater Process Technol 209:4830
11. Li YH, Housten W, Zhao YM et al (2007) Nanotechnology 18(20), Article No. 205607
12. Lahiri D, Bakshi SR, Keshri AK, Liu Y, Agarwal A (2009) Mater Sci Eng A Struct 523:263
13. Iijima S, Brabec C, Maiti A, Bernholc J (1996) J Chem Phys 104:2089
14. Falvo MR, Clary GJ, Taylor RM et al (1997) Nature 389:582
15. Kwon H, Park DH, Silvain JF, Kawasaki A (2010) Compos Sci Technol 70:546
16. Iijima S (1991) Nature 354:56
17. Treacy MMJ, Ebbesen TW, Gibson JM (1996) Nature 381:678
18. Ruoff RS, Lorents DC (1995) Carbon 33:925
19. Takesue I, Haruyama J, Kobayashi N et al (2006) Phys Rev Lett 96(5), Article No. 057001
20. Quang P, Jeong YG, Yoon SC, Hong SH, Kim HS (2007) J Mater Process Technol 187:318
21. Salas W, Alba-Baena NG, Murr LE (2007) Metall Mater Trans A 38A:2928
22. Morsi K, Esawi A (2007) J Mater Sci 42:4954. doi:10.1007/s10853-006-0699-y
23. Kuzumaki T, Miyazawa K, Ichinose H, Ito K (1998) J Mater Res 13:2445
24. Zhong R, Cong HT, Hou PX (2003) Carbon 41:848
25. Noguchi T, Magario A, Fukazawa S, Shimizu S, Beppu J, Seki M (2004) Mater Trans 45:602
26. Esawi AMK, El Borady MA (2008) Compos Sci Technol 68:486
27. Ci LJ, Ryu ZY, Jin-Phillipp NY, Ruhle M (2006) Acta Mater 54:5367
28. Pirgazi H, Akbarzadeh A, Petrov R, Sidor J, Kestens L (2008) Mater Sci Eng A Struct 492:110
29. Valiev RZ, Chmelik F, Bordeaux F, Kapelski G, Baudelet B (1992) Scripta Metall Mater 27:855
30. Kamikawa N, Tsuji N, Huang XX, Hansen N (2006) Acta Mater 54:3055
31. Tsuji N, Saito Y, Ito Y et al (2000) In: Symposium on ultrafine grained materials at the 2000TMS annual meeting, Mar 12–16, 2000, Nashville, TN, Ultrafine Grained Materials, pp 207–218
32. Ito Y, Tsuji N, Saito Y, Utsunomiya H, Sakai T (2000) J Jpn Inst Met 64:429
33. Lee SH, Saito Y, Tsuji N, Utsunomiya H, Sakai T (2002) Scripta Mater 46:281
34. Kamikawa N, Sakai T, Tsuji N (2007) Acta Mater 55:5873
35. Tsuji N, Ueji R, Ito Y, Saito Y (2000) In: Proceedings of the 21st RISØ international symposium on material science, p 607
36. Ashby MF (1970) Philos Mag 21:399
37. Iwahashi Y, Horita Z, Nemoto M, Langdon TG (1998) Acta Mater 46:3317
38. Keller TM, Laskoski M, Osofsky M, Qadri SB (2008) Phys Status Solidi A Appl Mater Sci 205:1585
39. Willems I, Konya Z, Colomer JF et al (2000) Chem Phys Lett 317:71
40. Hertel T, Walkup RE, Avouris P (1998) Phys Rev B 58:13870
41. Wang CY, Mioduchowski A (2007) J Appl Phys 101(1), Article No. 014306
42. Shen HS, Zhang CL (2007) Int J Solids Struct 44:1461
43. Deck CP, Flowers J, McKee GSB et al (2007) J Appl Phys 101(2), Article No. 023512
44. Tang DS, Chen LC, Wang LJ et al (2000) J Mater Res 15:560